



Evidence for active faulting in the eastern part of the Gulf of Saros, northern Aegean, from high-resolution seismic data

DENIZHAN VARDAR

Marine Geology and Geophysics Department, Institute of Marine Sciences and Management, Istanbul University, Istanbul, Turkey.

e-mail: denizhan@istanbul.edu.tr

MS received 16 April 2018; revised 22 June 2018; accepted 25 June 2018; published online 25 February 2019

This study focuses on the determination of the near-surface tectonic features in the eastern part of the Gulf of Saros, a highly active seismic region within the North Anatolian Fault Zone. Approximately 350-km-line high-resolution seismic data were acquired to understand the active tectonic setting of the inner side of the gulf. The Ganos Fault, which generated the 9 August 1912 earthquake ($M_w = 7.3$) in western Turkey, enters into the Gulf of Saros from the east, cuts the southern margin of the gulf forming a trough which becomes broader and deeper westward. The seismic data reveal that the fault is not made up of a single segment or a pair of border faults bounding the trough. According to the seismic images of the fault segments, however, the emanating earthquake energy will possibly be carried by two different faults; namely the Ganos and Saros segments. These fault segments will be presented first in this paper in detail from new collected seismic data at the inner part of the gulf, and will be used to help a new tectonic model that explains how the Ganos segment controls the northern margin of the trough while the Saros segment controls the central part of the main trough. The latter is responsible from the development of an active basin and it forms the sudden deepening observed on the trough.

Keywords. Gulf of Saros; high-resolution seismic; CHIRP seismic; ganos fault; saros fault.

1. Introduction

The Gulf of Saros is a NE–SW oriented basin that is located at the northeastern part of the Aegean Sea (figure 1a). It is a westward widening and deepening wedge-shaped embayment (>645 m) (Ustaömer *et al.* 2008) with a width of 30 km and a length of 55 km. The suggesting ages of the initial opening of the Gulf of Saros change from the Oligocene (Saner 1985; Coşkun 2000) to the Pliocene–Quaternary (Yaltırak 1996; Çağatay *et al.* 1998; Tüysüz *et al.* 1998; Yaltırak *et al.* 1998; Yaltırak and Alpar 2002). The basinal structure of the gulf is controlled by two main tectonic

forces: these are a NE–SW-trending strike-slip fault system at the western termination of the Ganos Fault and N–S extension of western Anatolia. The Ganos Fault (figure 1b) is regarded as the western continuation of the northern strand of the North Anatolian Fault Zone (NAFZ) (figure 1a).

After the destructive $M_w = 7.3$ earthquake triggered in 1912, the Ganos fault and other secondary faults have been studied and mapped by numerous researchers (Gutzwiller 1923; Ambraseys and Finkel 1987; Barka and Kadinsky-Cade 1988; Tüysüz *et al.* 1998; Yaltırak *et al.* 1998, 2000; Armijo *et al.* 1999, 2002, 2005; Okay *et al.* 1999, 2004; Kurt *et al.* 2000; Yaltırak and Alpar 2002;

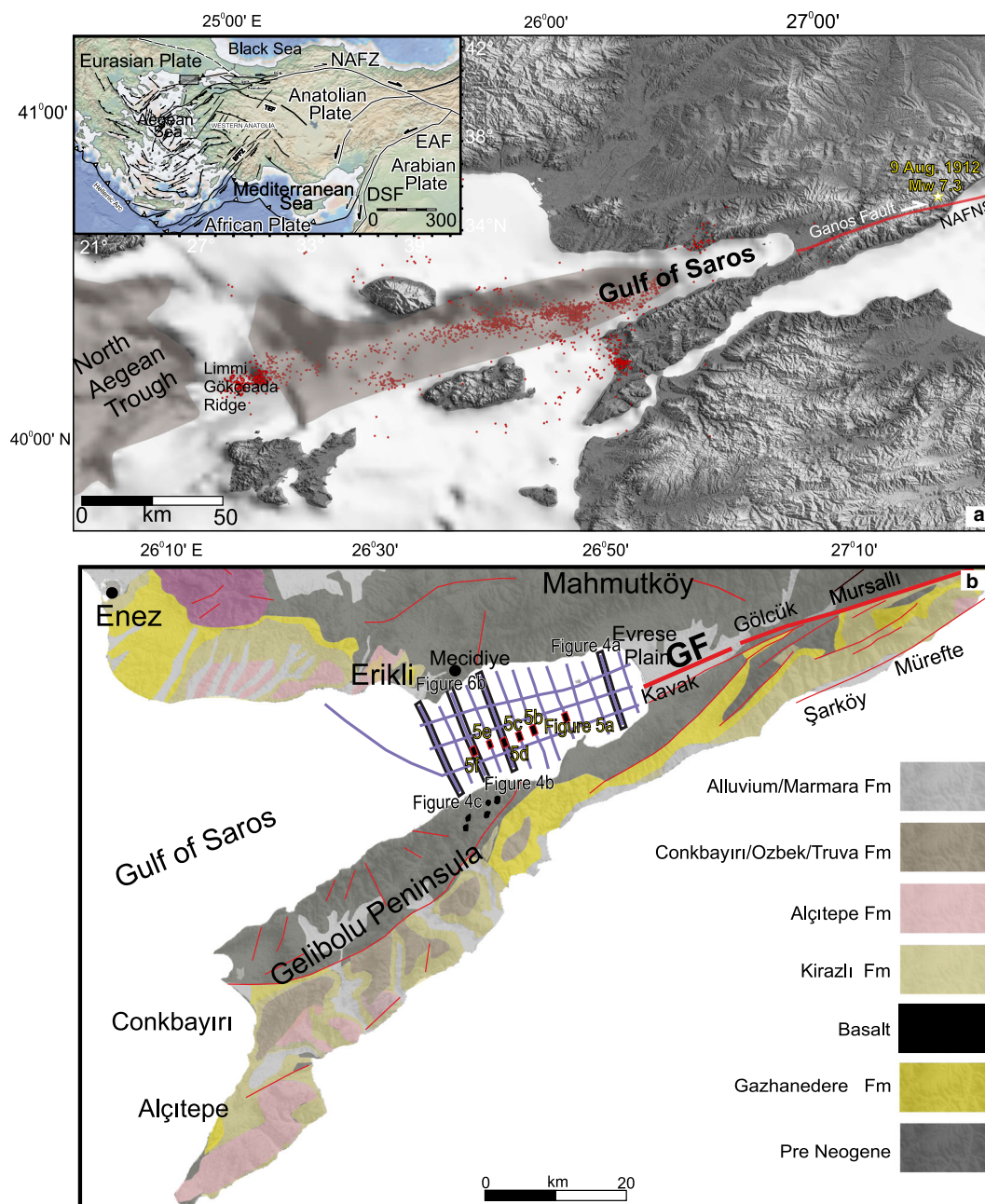


Figure 1. (a) Inset map shows generalised tectonics of Turkey, the seismicity map (1900–2016, koeri.boun.edu.tr) of North Aegean and Gulf of Saros (NAFNS), (b) the locations of the new seismic data superimposed on the geology map (Yaltrak *et al.* 1998).

Altınok *et al.* 2003; Altunel *et al.* 2004; Seeber *et al.* 2004; McNeill *et al.* 2004; Ustaömer *et al.* 2008). Altınok *et al.* (2003) estimated the total length of the surface rupture about 56 km, as extending NE–SW from Gaziköy to Gelibolu, with lateral slips ranging between 3.5 and 4.5 m.

The kinematical characteristics of the Gulf of Saros are still under debate and explained by three different tectonic models (figure 2); these are (a) an extension mechanism (Pfannenstiel 1944; Saner

1985), (b) a strike-slip mechanism (Barka and Kadinsky-Cade 1988; Görür *et al.* 1997; Çağatay *et al.* 1998; Tüysüz *et al.* 1998; Saatçılar *et al.* 1999; Kurt *et al.* 2000; McNeill *et al.* 2004) and finally (c) negative flower structure (transtension and transpression domains) model (Yaltrak 1996; Yaltrak *et al.* 1998; Yaltrak and Alpar 2002).

The discussions on the exact location of the Ganos Fault in the Gulf of Saros also continue. Some authors claim that it follows the southern

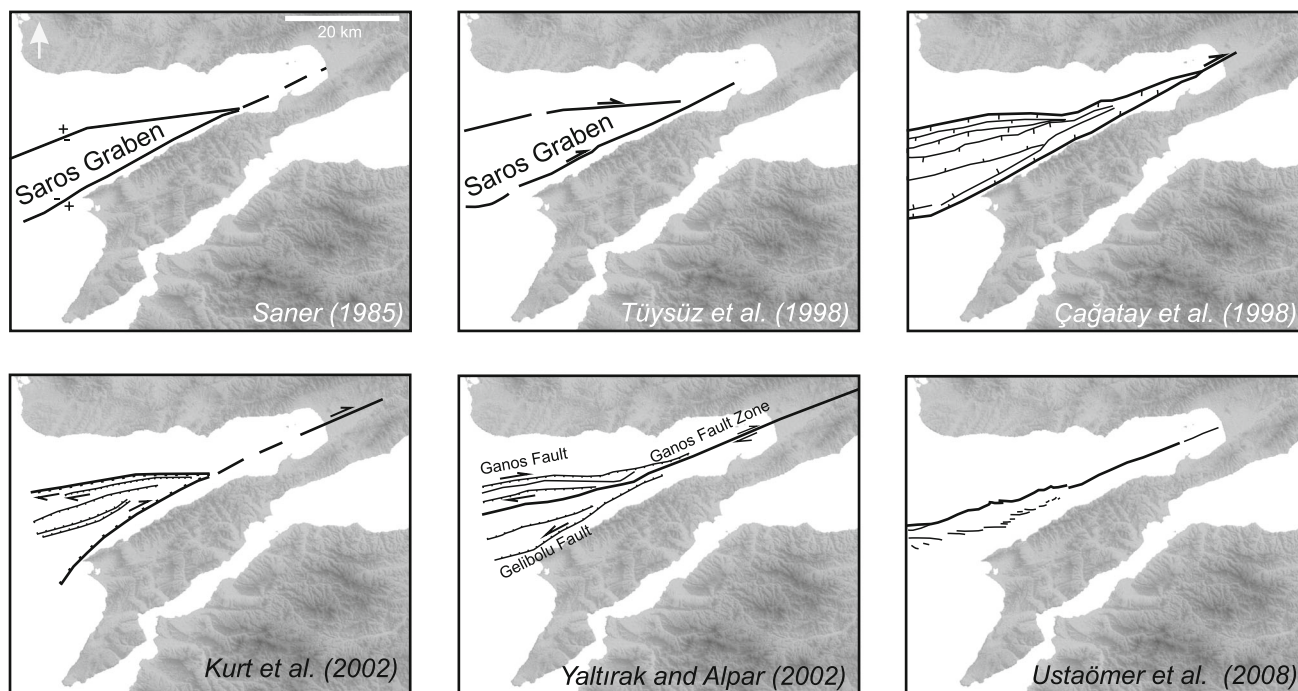


Figure 2. Selected previous fault models proposed for the Gulf of Saros (modified from Ustaömer *et al.* 2008).

margin of the main trough, while some others proposed that it is placed on the northern margin. Some other researchers suggested that it is divided into a number of segments at the eastern part of the gulf, so that they control the northern and southern boundaries. A geophysical study was performed by McNeill *et al.* (2004) who indicated the presence of right-lateral displacements with Riedel-type structures. In addition, Ustaömer *et al.* (2008) have shown that the Ganos Fault cuts the narrow deformation zone in the eastern gulf. Then it ended up on the slope. From this point onwards, it has been stated that the compressional forces formed two NE and SW oriented faults that cut the centre of the basin and formed Riedel-type faults.

The seismic data covering the Gulf of Saros is limited in order to demonstrate the active faulting within the inner gulf in detail. The available data are mainly distributed on the Aegean Sea exit of the gulf and there are only three seismic profiles (Çağatay *et al.* 1998; Yalırak *et al.* 1998; Ustaömer *et al.* 2008; Gökaşan *et al.* 2012) representing the eastern part. Three seismic profiles are not sufficient to understand the tectonic properties at the inner side of the gulf. The present study focuses on the eastern part of the gulf for determining detailed fault characteristics and types of the deformations that could be observed on shallow seismic data. For this purpose, new high-resolution seismic

profiles (figure 1b) were acquired at the eastern part of the Gulf of Saros in May 2016.

1.1 Geological setting

The 1500-km-long NAFZ is an intracontinental transform fault (Şengör 1979) and splits into three strands (Barka and Kadinsky-Cade 1988) at the eastern part of the Sea of Marmara (figure 1a). These branches terminate against the normal faults at the northern Aegean Sea where the westward escape of the Anatolian block turns into anticlockwise rotational wedges (Yalırak *et al.* 2012). All strands have different kinematic and seismic character in the region. The Northern Strand North Anatolian Fault Zone (NAFNS) enters the Sea of Marmara from Gulf of İzmit at the east, bounds the northern shelf of the Sea of Marmara, forming three major basins that reach the depth of over 1200 m, and finally connects to the Ganos Fault (Yalırak and Alpar 2002) at the west (figure 1a).

The most dominant unit in the stratigraphy of the surrounding onshore area of the Gulf of Saros is the Pre-Miocene and young sedimentary volcanic sequences (Ustaömer *et al.* 2008) (figure 1b). Four major unconformities were defined in the Tertiary–Quaternary evolution, representing dominant tectonic events, erosions and sedimentation periods (Saner 1985; Sümengen *et al.* 1987; Yalırak 1996).

These unconformities constitute the bases of the Pre-Miocene, Miocene, and Pliocene and Quaternary sequences. The Gazahandere, Kirazlı, Alçitepe (Miocene units) formations that are mainly overlain unconformably by younger units, outcrop along the shores of the Çanakkale Strait and between the towns of Enez and Erikli. The Miocene sedimentary sequences show some facies differences in the Thrace and Gelibolu peninsulas (Saner 1985; Sümengen *et al.* 1987; Yaltrak 1996; Sakiç *et al.* 1999). The sequence was initially deposited as a lacustrine unit in the Gelibolu Peninsula and then it was deposited as a lacustrine and a marine unit at the same time in the peninsula of Thrace (Sümengen *et al.* 1987). The Pliocene units (Conkbayırı, Ozbek and Truva formations) are observed at the southern part of the Gelibolu Peninsula. The alluvium formations form the current geology of the marine and river basins and the alluvial reservoir work area of the modern river.

2. Material and methods

A total of 350 km high-resolution shallow seismic reflection data have been collected and interpreted in order to determine the structural signatures of the eastern part of the Gulf of Saros (figure 1b). Chirp data were acquired by using a Bathymetry 2010P™ Chirp sub-bottom profiler and bathymetric echo sounder with four transducers, each producing 2–8 kHz Chirp signals. The power level, sweep bandwidth and detection threshold were adjusted automatically during the survey. The transmit pulse repetition rate was dependent on the depth range. The survey speed was fixed to 3.5–4.0 knot during the survey. Gain correction, band-pass filter (10/15–1750/1900 Hz) and predictive deconvolution were applied to Chirp data. These data were processed using Kogeo Seismic Toolkit 2.7 and analysed by ‘The Kingdom Suite’ software.

Some of the available vintage seismic profiles (sparker), navigated with short-range position fixing, were also considered, even though they are expected to have positional errors. In this study, the navigation data were recorded with the Magellan Proflex 500 scientific GPS system with a horizontal error margin of about ± 10 cm, and the same positioning information stored in the headers of seismic data files.

The bathymetry map (figure 3b) constitutes three data sets: (a) sea-bottom depth data acquired

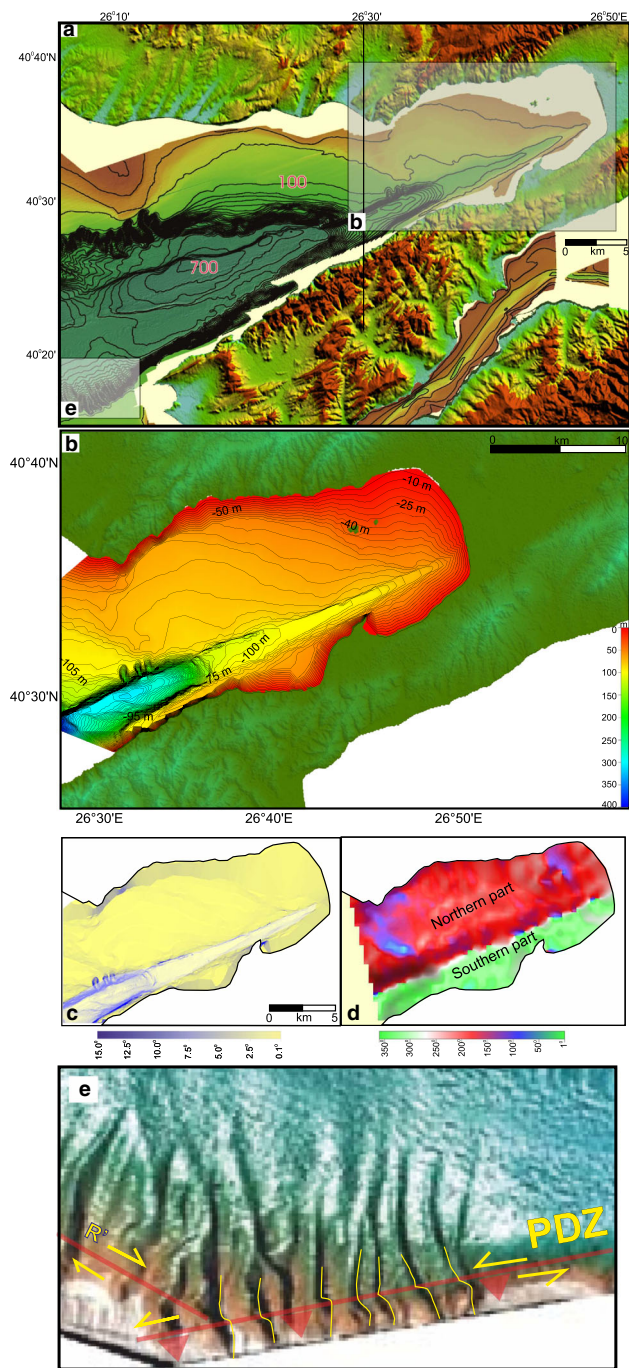


Figure 3. (a) The multibeam bathymetry map from Ustaömer *et al.* (2008) and Gökaşan *et al.* (2010) and land topography map of the Gulf of Saros; (b) the bathymetry map of the study area and merged from seismic data used in this study, ETOPO 1 and digitised charter maps data); (c) the slope map of the gulf; (d) the slope direction map of the gulf; and (e) zoomed view of the multibeam bathymetry that shows submarine canyons and offsets (R: Riedel fault; PDZ: principal displacement zone).

from seismic profiles; (b) ETOPO 1 data (Amante and Eakins 2009); and (c) digitised charter maps (e.g., Navionics). All the data merged in ARCGIS

program as a shape file changed to DEM (Digital Elevation Model) file in ENVI program. The final figure (figure 3b) was shaded in GLOBAL Mapper program.

3. Results

3.1 The morphology of the study area

The Ganos Fault enters into the Gulf of Saros from the eastern termination of the gulf (figure 1b); it cuts the southern part of the gulf and forms a trough deepening westward (figure 3a and b). It is the trough that divides the gulf into two (figure 3a and b). The gentle wall slopes of the trough (i.e., $1-2^\circ$) increases up to $10-12.5^\circ$ in front of the Town Mecidiye (figure 3c). The slope of the basin floor is 0.5° and ascends to the front of the Mecidiye with 7.5° slope (figure 3d). The seafloor depths of the trough change from -100 to -300 m (figure 3b) with respect to the slope. The most prominent feature of the slope direction map of the gulf is two partial structures and fault controlled lineament (figure 3d).

3.2 Structural interpretation of the high-resolution seismic data

The main fault system that controls the common structural and morphological properties of the gulf can be clearly followed on the high-resolution shallow seismic profiles (figure 4a–c). The main fault system (f1), namely the Ganos Fault, cuts the northern margin (figure 3b) of the basin (figure 4a) at the eastern part of the gulf. The slope gradient of the stratified sedimentary packages in the trough changes $1-9^\circ$ (figure 4a). The fault ‘f1’ is parallel to the Ganos Fault to the NW, but contrarily it does not affect the sea floor (figure 4a). The uplift of the acoustic basement at the northern (figure 4a) and southern parts (figure 4a–c) of the study area is noteworthy. The uplift causes normal faulting (fn) (figure 4a) at the northeastern part of the gulf. ‘f2’ fault can be observed roughly parallel to the ‘f1’ fault to the west. These two faults are both affected by the sea floor at the centre and the western part of the study area (figure 4a and b) and cause a small extension that can be traced at the centre of the study area (figure 4b). This is one of the most important proofs for the current activity.

A new fault (f3) appears in the sudden deepening part of the trough where ‘f1 and f2’

vanish westward (figure 4c). It is more deformed if compared to the faults f1 and f2, because it is the most important tectonic element responsible for the abrupt deepening morphology of the gulf (figure 4c). According to the offsets on the submarine canyons (figure 3e) that can be observed at the western outlet of the Gulf of Saros, the fault f3 has left-lateral movement. The step between the faults f1 and f3 possibly occurred due to different oblique movements of the blocks. Therefore, they seem to be different segments depending on their characteristic properties. This fault is covered by sediment at the places where the trough deepens suddenly (figure 4c). The extension and the new fault evaluation (f2) are possibly controlled by the southwestern movement of the southern block.

The terraces observed in the study area (figure 4a–c) are mainly controlled by the faults. The sea-level changes and the sedimentary depositions play some secondary roles. The trough is possibly covered by the sea during the global lowstand period. The sedimentary input into the southern part of the gulf is believed to be relatively lower than that at the northern part, causing the unconformity surfaces observed at the southern margin.

4. Discussion and conclusion

The sea floor topography of the eastern part of the Gulf of Saros is commonly controlled by main structural elements. The slope of the main trough and the trend of its direction increase to the west. The slope and slope orientation maps (figure 4d and e) indicate that the tectonic settings of the northern and southern parts of the gulf exhibit different characteristics. The fault f1 (Ganos Fault) enters the eastern part of the gulf that formed the trough which can be easily outlined from the seismic profiles (figure 5a–e). The fault is also shown by Çağatay *et al.* (1998, their figure 5). The length of Ganos Fault is about 20 km within the gulf. The fault f2 appears parallel to the fault f1 at the central part of the study area. ‘f1’ and ‘f2’ faults together form a small passage. A new transform fault (f3), which is identified and named as the Saros Fault in this study (figure 5f), is controlling the general morphology of the gulf. The sudden deepening of the trough occurred under the control of the Saros Fault where the Ganos Fault lost its activity (figure 5f). Both the morphological properties of the sea floor and the new

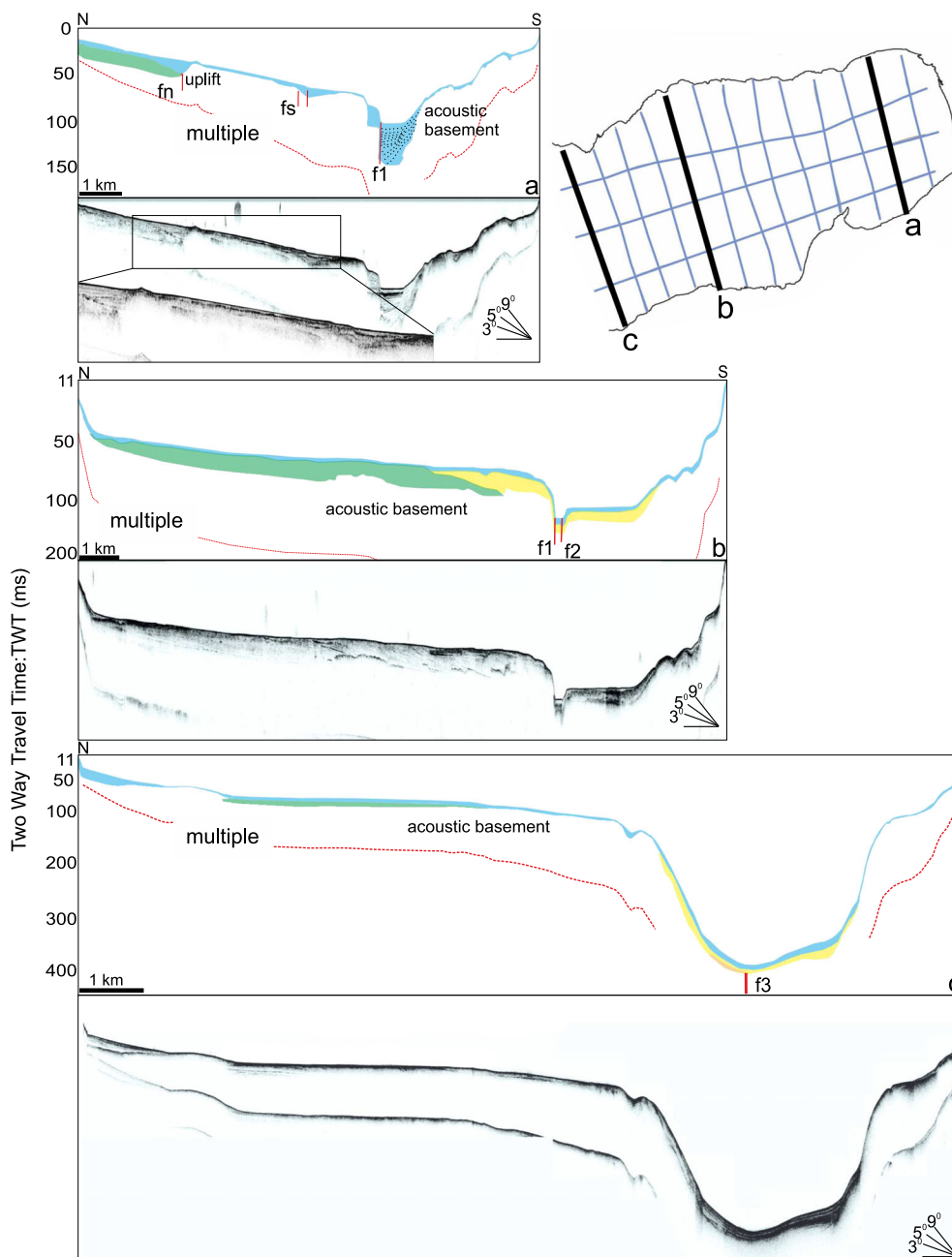


Figure 4. The interpreted–non–interpreted high–resolution seismic profiles and locations. Red dashed lines are multiple reflections. 1–9° arrows show the real slopes calculated by Kingdom Suite (2.7). The faults fn, fs, f1, f2 and f3 are observed in the seismic profiles. See figure 1(b) for their locations.

steeper and deeper basin formation traced from the seismic sections (figures 4 and 5) indicate an extensional mechanism was dominant in the study area. According to the offsets observed on the submarine canyons at the western outlet of the gulf, the fault SF is left lateral where the fault GF is right lateral. These differential movements cause an extension mechanism at the study area and probably the fault f2 was formed because of these two tectonic forces. According to the morphological view of the

small passage that formed between the faults f1 and f2 the initial phase of the extension tectonics dominated in the study area.

Although the seismicity map shows seismic gap at the eastern part of the Gulf of Saros (figure 1a), Karabulut *et al.* (2006) proposed 40–50 km long submarine segment in the Gulf of Saros because the northeastern termination of the aftershock sequence could be accepted as the western termination of the 1912 earthquake rupture. The fault

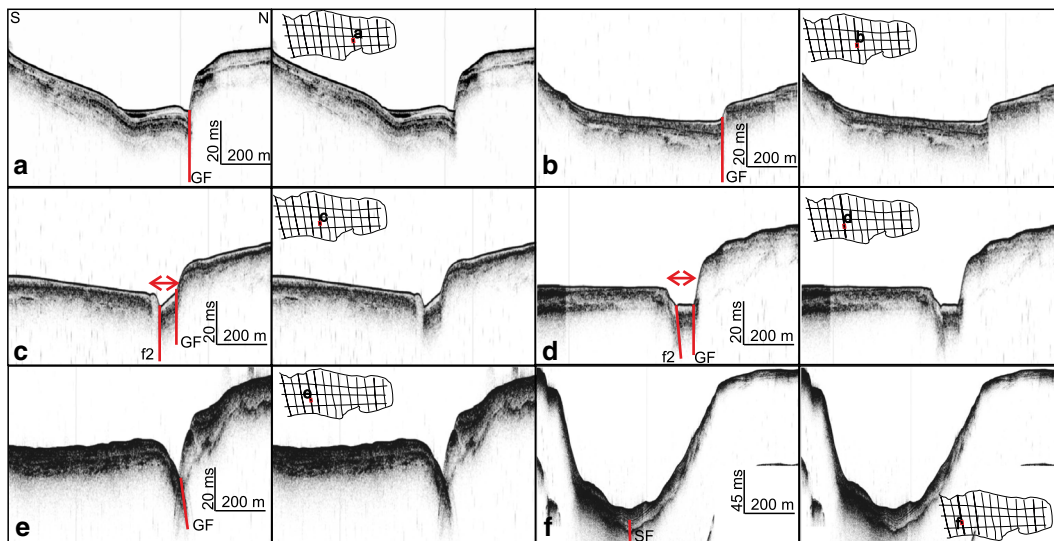


Figure 5. The zoomed seismic lines show active faulting at the Gulf of Saros (GF: Ganos Fault; SF: Saros Fault). The horizontal two-sided arrows show the extension movements. See also figure 1(b) for locations.

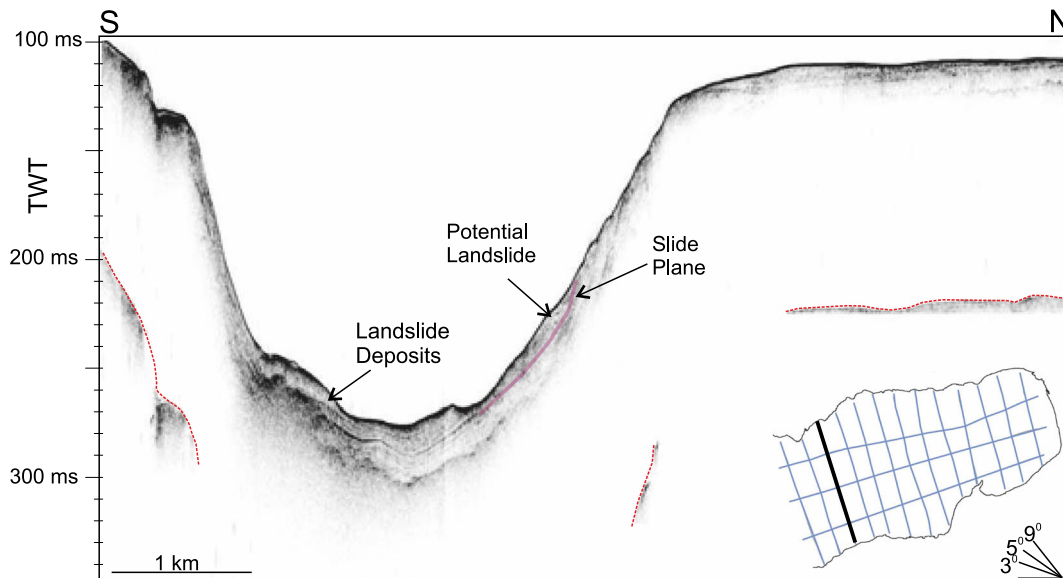


Figure 6. Seismic profile showing landslide deposits, potential landslides and the slide plane.

settings obtained in this study, those with evidently traceable surface lineation, support their finding (figures 4a, b and 5a-e). The surface effects cannot be observed at the westernmost part of the study area because of the sedimentary deposits (figures 4c and 5f).

The sedimentary deposits cover the surface fractures of the Saros Fault at the western part of the trough where the basin slope increases suddenly (figures 5f and 6). Their reflection characteristics and terminations indicate that they are landslide deposits (figures 5f and 6), which might be moved by the recent earthquakes. The higher

slopes of the gulf (slide planes) observed on the seismic data (figure 6) probably cause mass movements during the earthquakes. It is well known that strike-slip earthquakes may not cause tsunamis, but mass movements occurring during these earthquakes may cause landslide triggered tsunamis (Yalçiner *et al.* 2002). Therefore, the coastal areas near the North Aegean Trough are under the threat of tsunami risk because of the possible submarine landslide areas (see also Altınok *et al.* 2011, 2013 for Aegean tsunamis). In view of this threat, an estimation of seismic risk of this area should be carried out by modern techniques, i.e., the

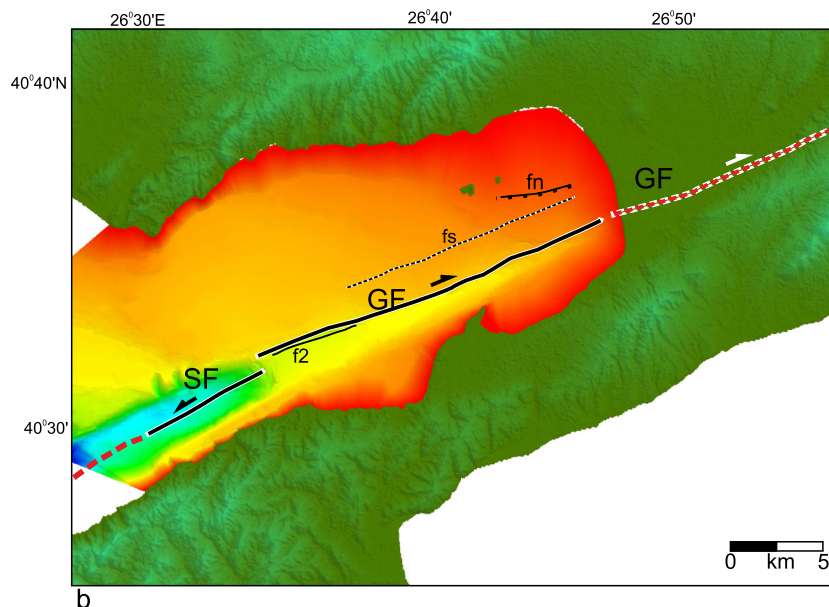


Figure 7. Fault map of the eastern part of the Gulf of Saros. The *fn* is a normal fault near the islands, while the *fs* is a 16-km-long inactive transform fault. GF: Ganos Fault; SF: Saros Fault.

nowcasting approach (Rundle *et al.* 2018) which is based on the use of a new time domain termed natural time (Varotsos *et al.* 2005, 2011).

The inactive faults *fs* and *fn* are also determined in the study area (figure 7). The fault *fs* extends approximately 16 km parallel to the Ganos Fault (figure 7). On the other hand, the fault *fn* is observed only at the eastern part of the study area near the islands.

The previous fault maps of the gulf were constructed by interpreting the multi-beam bathymetry maps, and confirmed by the analogue seismic sections (Çağatay *et al.* 1998; Yalırak *et al.* 1998; Ustaömer *et al.* 2008; Gökaşan *et al.* 2012). On the other hand, because of the large intervals between the available seismic sections, it was not easy to determine the changes in the fault characters. The new high-resolution seismic data show that the main fault system of the eastern part of the gulf is not made up of a one-piece segment (Ustaömer *et al.* 2008; Gökaşan *et al.* 2012) or bounded by two boundary faults (Çağatay *et al.* 1998; Yalırak *et al.* 1998). The fault energy is carried by two fracture mechanisms (figure 7a). At first, the Ganos Fault affects the northern margin of the trough (figure 7), before the younger Saros Fault passing through the trough's centre. The Saros Fault causes the active formation of a new basin and the steep deepening of the trough (figure 7). The new basin was possibly formed as the result of the southwestern move of the southern part that creates the Saros Fault, and

causes deepening of the basin (figure 7). According to the gravity inversion study derived from the satellite gravity data (Tirel *et al.* 2004), the North Aegean Trough is related with a two-stage evolution of the Aegean extension.

Acknowledgements

This work was supported by the Scientific Research Projects Coordination Unit of Istanbul University, project numbers YADOP-51794 and BEK-2017-24925. The author also appreciates the help that Sinan Demirel and Özkan Çamurcu gave during marine data acquisition, and the contributions of Bedri Alpar and Hakan Alp to data interpretation.

References

- Altınok Y, Alpar B and Yalırak C 2003 Şarköy–Mürefte 1912 earthquake's tsunami extension of the associated faulting in the Marmara Sea, Turkey; *J. Seismol.* **7** 329–346.
- Altınok Y, Alpar B, Özer N and Aykurt H 2011 Revision of the tsunami catalogue affecting Turkish coasts and surrounding regions; *Nat. Hazard. Earth Syst.* **11** 273–291.
- Altınok Y, Alpar B, Yalırak C, Kıyak N G and Zabcı C 2013 Tsunami effects on the eastern coast of Saros Bay, Turkey; In: *Proceedings of the 40th CIESM Congress*, Marseille, pp. 40–42.
- Altunel E, Meghraoui M, Akyüz H S and Dikbas A 2004 Characteristics of the 1912 co-seismic rupture along the North Anatolian Fault Zone (Turkey): Implications for the expected Marmara earthquake; *Terra Nova* **16** 198–204.

- Amante C and Eakins B W 2009 ETOPO1 1 arc-minute global relief model: Procedures, data sources and analysis; NOAA Technical Memorandum NESDIS NGDC-24, National Geophysical Data Center, NOAA, <https://doi.org/10.7289/V5C8276M>.
- Ambraseys N N and Finkel C F 1987 The Saros–Marmara earthquake of 9 August 1912; *Earthq. Eng. Struct. Dyn.* **15** 189–211.
- Armijo R, Meyer B, Hubert A and Barka A 1999 Westward propagation of the North Anatolian Fault into the northern Aegean: Timing and kinematics; *Geology* **27** 267–270.
- Armijo R, Meyer B, Navarro S, King G and Barka A 2002 Asymmetric slip partitioning in the Sea of Marmara pull-apart: A clue to propagation process of the North Anatolian Fault; *Terra Nova* **14** 80–86.
- Armijo R, Pondard N, Meyer B, Uçarkuş G, Mercier de Lépinay B, Malavieille J, Dominguez S, Gustcher M, Schmidt S, Beck C, Çağatay N, Çakır Z, İmren C, Eriş K, Natalin B, Özalaybey S, Tolun L, Lefèvre I, Seeber L, Gasperini L, Rangin C, Emre O and Sarıkavak K 2005 Submarine fault scarps in the Sea of Marmara pull-apart (North Anatolian Fault): Implications for seismic hazard in Istanbul; *Geochem. Geophys. Geosys.* **6** 1–29.
- Barka A A and Kadinsky-Cade K 1988 Strike-slip fault geometry in Turkey and its influence on earthquake activity; *Tectonics* **7** 663–684.
- Çağatay N, Görür N, Alpar B, Saatçılar R, Akkök R, Sakıncı M, Yüce H, Yaltırak C and Kuşçu İ 1998 Geological evolution of the Gulf of Saros, NE Aegean Sea; *Geo-Mar. Lett.* **18** 1–9.
- Coşkun B 2000 North Anatolian Fault–Saros Gulf relationships and their relevance to hydrocarbon exploration, northern Aegean Sea, Turkey; *Mar. Pet. Geol.* **17** 751–772.
- Gökaşan E, Tur H, Ergin M, Görüm T, Batuk F G, Sağci N, Ustaömer T, Emem O and Alp H 2010 Late Quaternary evolution of the Çanakale Strait region (Dardanelles, NW Turkey): Implications of a major erosional event for the postglacial Mediterranean–Marmara Sea connection; *Geo-Mar. Lett.* **30** 113–131.
- Gökaşan E, Görüm T, Tur H and Batuk F G 2012 Morphotectonic evolution of the Çanakale Basin (NW Anatolia): Evidence for a recent tectonic inversion from transpression to transtension; *Geo-Mar. Lett.* **32** 227–239, <https://doi.org/10.1007/s00367-011-0262-y>.
- Görür N, Çağatay M N, Sakıncı M, Sümengen M, Şentürk K, Yaltırak C and Tchapyalga A 1997 Origin of the Sea of Marmara as deduced from the Neogene to Quaternary paleogeographic evolution of its frame; *Int. Geol. Rev.* **39** 342–352.
- Gutzwiller O 1923 Beitrage zur Geologie der Umgebung von Merfete (Mürefte) am Marmara Meer; PhD Thesis, Universität Basel, Basel, 347p.
- Karabulut H, Roumelioti Z, Benetatos C, Mutlu A K, Özalaybey S, Aktar M, and Kiratzi A 2006 A source study of the 6 July 2003 (Mw 5.7) earthquake sequence in the Gulf of Saros (Northern Aegean Sea): Seismological evidence for the western continuation of the Ganos fault; *Tectonophysics* **412**(3–4) 195–216.
- Kurt H, Demirbağ E and Kuşçu I 2000 Active submarine tectonism and formation of the Gulf of Saros, NE Aegean Sea, inferred from multi-channel seismic reflection data; *Mar. Geol.* **165** 13–26.
- McNeill L C, Mille A, Minshull T A, Bull J M, Kenyon N H and Ivanov M 2004 Extension of the North Anatolian Fault into the North Aegean Trough: Evidence for transtension, strain partitioning, and analogues for Sea of Marmara basin models; *Tectonics* **23** 1–42.
- Okay A, Demirbağ E, Kurt H, Okay N and Kuşçu I 1999 An active, deep marine strike-slip basin along the North Anatolian fault in Turkey; *Tectonics* **18** 129–147.
- Okay A I, Tüysüz O and Kaya Ş 2004 From transpression to transtension: Changes in morphology and structure around a bend on the North Anatolian Fault in the Marmara region; *Tectonophysics* **391** 259–282.
- Pfannenstiel M 1944 Diluviale Geologie des Mittelmeergebietes, die diluvialen Entwicklungsstadien und die Urgeschichte von Dardanellen, Marmara Meer und Bosphorus; *Geol. Rundsch.* **34** 334–342.
- Rundle J B, Luginbuhl M, Giguere A L and Turcotte D 2018 Natural time, nowcasting and the physics of earthquakes: Estimation of seismic risk to global megacities; *Pure Appl. Geophys.* **175** 647–660.
- Saatçılar R, Ergintav S, Demirbağ E and İnan S 1999 Character of active faulting in the North Aegean Sea; *Mar. Geol.* **160** 339–353.
- Sakıncı M, Yaltırak C and Oktay F Y 1999 Palaeogeographical evolution of the Thrace Neogene Basin and the Tethys–Paratethys relations at northwestern Turkey (Thrace); *Palaeogeogr. Palaeoclimatol. Palaeoecol.* **153** 17–40.
- Saner S 1985 Sedimentary sequences and tectonic setting of Saros Gulf region NE Aegean Sea, Turkey; *Bull. Geol. Soc. Turkey* **28** 1–10.
- Seeber L, Emre O, Cormier M H, Sorlien C C, McHugh C M G, Polonia A, Ozer N and Çağatay N 2004 Uplift and subsidence from oblique slip: The Ganos–Marmara bend of the North Anatolian Transform, western Turkey; *Tectonophysics* **391** 239–258.
- Şengör A M C 1979 The North Anatolian Transform Fault: Its age offset and tectonic significance; *J. Geol. Soc. London* **136** 269–282.
- Sümengen M, Terlemez I, Şentürk K, Karaköse C, Erkan E, Ünay E, Gürbüz M and Atalay Z 1987 Stratigraphy, sedimentology, and tectonics of the Tertiary sequences in Gelibolu Peninsula and southwestern Thrace; Bulletin of the Mineral Research and Exploration Institute of Turkey Technical Report 8128 (in Turkish), 260p.
- Tirel C, Gueydan F, Tiberi C and Brun J P 2004 Aegean crustal thickness inferred from gravity inversion. Geodynamical implications; *Earth Planet. Sci. Lett.* **228** 267–280.
- Tüysüz O, Barka A A and Yiğitbaş E 1998 Geology of the Saros Graben: Its implications on the evolution of the North Anatolian Fault in the Ganos–Saros Region, NW Turkey; *Tectonophysics* **293** 105–126.
- Ustaömer T, Gökaşan E, Tur H, Görüm T, Batuk F, Kalafat D, Alp H, Ecevitoglu B and Birkan H 2008 Faulting, mass-wasting and deposition in an active dextral shear zone, the Gulf of Saros and the NE Aegean Sea, NW Turkey; *Geo-Mar. Lett.* **28** 171–193.

- Varotsos P A, Sarlis N V, Tanaka H K and Skordas E S 2005 Some properties of the entropy in natural time; *Phys. Rev. E* **71** 032102.
- Varotsos P A, Sarlis N and Skordas E S 2011 Entropy in natural time; In: *Natural time analysis: The new view of time* Springer Praxis Books. Springer, Berlin, Heidelberg, pp. 159–187.
- Yaltırak C 1996 Ganos Fay Sisteminin tektonik tarihi; *TPJD Bult.* (in Turkish) **8** 137–156
- Yalçınmer A C, Alpar B, Altınok Y, Özbay İ and Imamura F 2002 Tsunamis in the Sea of Marmara: Historical documents for the past, models for the future; *Mar. Geol.* **190** 445–463.
- Yaltırak C and Alpar B 2002 Kinematics and evolution of the northern branch of the North Anatolian Fault (Ganos Fault) between the Sea of Marmara and the Gulf of Saros; *Mar. Geol.* **190** 351–366.
- Yaltırak C, Alpar B and Yüce H 1998 Tectonic elements controlling the evolution of the Gulf of Saros (north-eastern Aegean Sea, Turkey); *Tectonophysics* **300** 227–248.
- Yaltırak C, Alpar B, Sakıncı M and Yüce H 2000 Origin of the Strait of Çanakkale (Dardanelles): Regional tectonics and the Mediterranean Marmara incursion; *Mar. Geol.* **164** 139–159.
- Yaltırak C İşler E B, Aksu A E and Hiscott R N 2012 Evolution of the Bababurnu Basin Peninsula: Western extension of the middle strand of the North Anatolian Fault Zone, Northeast Aegean Sea, Turkey; *J. Asian Earth Sci.* **57** 103–119.

Corresponding editor: ARKOPROVO BISWAS